Research Article   **Open Access**

Discovery of Small Molecule TLR4 Inhibitors as Potential Therapy for Alzheimer's Disease

Vemulapalli Sindhu

Vista del Lago
Email: sindhuv0322@gmail.com

ABSTRACT

Alzheimer's is a potent neurodegenerative disease that causes cognitive decline. Microglia are phagocytes in the brain that can play a role in cell death and neuroinflammation, leading to Alzheimer's. Microglia have surface receptors that activate them when ligated, and one such receptor is toll-like receptor 4 (TLR4) which this research focuses on inhibiting. By identifying compounds that obstruct the pathway between TLR4 and microglia, the neuroinflammatory response associated with microglial activation in neurodegenerative diseases will be reduced. Although experiments targeting TLR4 inhibition have been performed, this paper employs a novel approach by using a database of 20 million compounds for virtual screening to identify a suitable target compound, overcoming limitations in past studies. To execute the drug discovery process, TLR4's binding sites were identified using a geometric, energetic, and machine-learning approach. Then, pharmacophore maps were created and virtual screening was conducted to identify 20 compounds that could inhibit TLR4. The 10 molecules with the most favorable Gibbs Free Energy were selected and their absorption and toxicity were tested. This process yielded one promising compound as a TLR4 and Alzheimer's antagonist.

Keywords: TLR4, Drug discovery, Alzheimer's Disease, Neuroinflammation, Virtual screening

1. INTRODUCTION:

Alzheimer's, a progressive neurodegenerative disease that is caused by damage to neurons, is the fifth-leading cause of death in Americans ages 65 and older (Centers for Disease Control and Prevention, 2020). From 2000 to 2019, deaths stemming from Alzheimer's disease (AD) increased by more than 145%, and, by 2050, AD cases are expected to triple globally (Alzheimer's Disease Facts and Figures, 2023; Scheltens et al., 2021; Centers for Disease Control and Prevention, 2020). In 2020, 5.8 million Americans were living with AD and the risk of developing this disease has been shown to increase with age (Scheltens et al., 2021). With Alzheimer's prevalence, the causes and

effects of the disease are critical to understand for therapeutic methods to be developed.

AD is characterized by plaque buildup and neurofibrillary tangles (NFTs) (Hur, 2022). Different theories regarding AD pathology exist, with the amyloid hypothesis being one of the most prevalent. The amyloid hypothesis states that the misfolding of extracellular β-amyloid (Aβ) protein accumulated in plaques and misfolded intracellular tau protein in NFTs leads to AD (Chen et al., 2017).

Abnormally aggregated Aβ and tau aggregates, which cause NFTs, affect neuroinflammation and synapse loss caused by activated microglia (Bamberger et al., 2003). "Neuroinflammation" refers to a pro-inflammatory response in the central nervous system (CNS) that occurs as glial cells including microglia mobilize in response to an injury (Glass et al., 2010). Microglia are vital to immune responses, but their role in responding to injurious stimuli by activating an inflammatory pathway can exacerbate AD (Yang et al., 2020; Al-Ghraiybah et al., 2022).

As resident phagocytes of the CNS, microglia can clear the brain of pathogens and contribute to synaptic protection (Al-Ghraiybah et al., 2022). The phenotype that microglia develop is dependent on the stimuli present; they can develop the M1 phenotype which has pro-inflammatory functions or the M2 phenotype which has anti-inflammatory functions. When activated by pathological triggers like protein aggregates, microglia migrate to the injury site and initiate an immune response by recognizing danger-associated or pathogen-associated molecular patterns (DAMPs/PAMPs) via specific receptors (Kwon and Koh, 2020). In AD, microglia bind to Aβ oligomers through receptors such as toll-like receptor 4 (TLR4). This leads to a phenotypic change as microglia become pro-inflammatory, inducing the production of cytokines and chemokines which contribute to the inflammation and neuronal loss in AD (Wu et al., 2022; Ciesielska et al., 2021).

Microglia are activated through receptors on their surface such as TLR4, a pattern-recognition receptor essential to the immune response (Akira et al., 2006; Płóciennikowska et al., 2015). TLR4 is activated by lipopolysaccharides (LPS) through binding facilitated by the MD-2 protein, forming the TLR4/MD-2/LPS complex (Calvo-Rodriguez et al., 2020). This complex triggers downstream signaling pathways, primarily through the adaptor protein myeloid differentiation factor 88, resulting in the activation of NF-κB. TLR4/ NF-κB is a critical transcription factor in microglia that upregulates several M1 genes encoding cytokines, growth factors, and other inflammatory mediators (Duan et al., 2022; Mangalmurti and Lukens, 2022). Additionally, TLR4 can be activated by damage-associated molecular patterns (DAMPs) (Ciesielska et al., 2021). When microglia are activated, pro-inflammatory cytokines including tumor necrosis factor-α (TNF-α) and interleukin-6 (IL-6) increase as do cytosolic Ca2+ concentrations in neurons (Rajesh and Kanneganti, 2022). This increase in Ca2+ levels triggered by TLR4 activation leads to necroptosis and mitochondrial Ca2+ overload, accelerating neuro-degeneration (Zusso et al., 2019; Akira et al., 2006). Necroptosis, an inflammatory form of cell death that releases intracellular contents acting as DAMPs, is triggered by the ligation of receptors such as TLR4, leading to a positive feedback cycle (Płóciennikowska et al., 2015).

2. MATERIALS AND METHODS

2.1. Analysis of binding sites in TLR4
2.1.1 DoGSiteScorer
DoGSiteScorer is a platform that analyzes protein-ligand complexes (Volkamer et al., 2012). Specifically, it determines binding sites by identifying surface regions that are clustered based on geometric continuity. These areas are scored based on volume, depth, and surface area to evaluate their potential as binding sites, and information such as volume, surface area, and scores are displayed.

To obtain the desired results, navigate to DoGSiteScorer, enter the PDB code (an identifier specific to each protein), and press the "Go" button. Several computational tools will appear next to a 3D model of the protein, with DoGSiteScorer as the second option. Click it, adjust any analysis settings, and click "Calculate." A table will appear and binding sites can be highlighted by pressing the eye icon. Information including the drug score indicating the site's drug-binding efficacy is shown.

2.1.2 FTSite
FTSite uses an energy-based method to determine protein binding sites, calculating the energies between

molecules and the protein surface and identifying potential binding sites (Ngan et al., 2012).

To generate information via FTSite, enter the "Job Name", the PDB code, the chain of interest, and optionally an email address to which results will be sent. Press "Find My Binding Site" and, once the results are ready, a 3D structure of the protein and the identified binding sites will be displayed.

2.1.3 PrankWeb

PrankWeb is a website that models protein-ligand binding sites using machine-learning to predict binding sites based on chemical areas around the protein surface (Jendele et al., 2019).

After entering the PrankWeb website, enter the PDB code and adjust the settings—such as selecting which chains to investigate by unselecting the "original structure" box— and click "Submit" to generate binding sites. A 3D model of the protein with the sites highlighted will appear along with the sequence of amino acids composing the protein and a table of information about the clusters.

2.2 Pharmacaphore Maps and Virtual Screening
2.2.1 Druggable Cluster Identification Using Pocket Query

PocketQuery is a website that uses PDB codes to identify druggable protein clusters. The amino acid residues composing the cluster, maximum cluster distance, and cluster score are displayed (Koes and Camacho, 2012a).

On PocketQuery, enter the PDB code in the "ID" box and click "Search." A table with the above data will appear, and clicking on each row will show the molecular structure and residues.

2.2.2 Virtual Screening through ZINCPharmer

ZINCPharmer is a web interface that virtually screens compounds in the ZINC database using the clusters generated by PocketQuery. Pharmacophore maps that highlight the key interaction and spatial features of the compounds are created, enabling the identification of potential small molecule drug candidates that can fit with the chosen pharmacophore classes (Koes and Camacho, 2012b).

On PocketQuery, click on the "Export" tab towards the bottom of the page. Click "Send to ZINCPharmer" so that the cluster selected is analyzed in ZINCPharmer.

Once on ZINCPharmer, click to the "Viewer" tab and unselect the "Visible" checkboxes under the "Ligand" and "Receptor Residues" sections for clarity. Go back to the "Pharmacophore" tab and under the "Enabled" column, unhighlight the checkboxes for the pharmacophore classes such that at least three classes of interest remain. Click "Submit Query" and press "RMSD" twice to sort from lowest to highest RMSD scores. Select the compounds with the lowest RMSD scores after testing multiple clusters and classes.

2.3 Molecular Docking through SwissDock

SwissDock is an online tool that models interactions between small molecules and target proteins. The protein and molecule interaction structures and Gibbs Free Energy, which is denoted as the "SwissParam Score," are amongst the outputted data (Bugnon et al., 2024; Röhrig et al., 2023).

After navigating to the SwissDock website, enter the SMILES format for the small molecule. The SMILES identifier can be obtained from a database containing chemical properties of molecules called PubChem (PubChem, 2024). Then, press "Prepare Ligand." After confirming that a green checkmark has appeared, move on to step 2: "Submit a target." Enter the PDB code, press "Enter," select which chains of the protein to model, select the heteroatoms to keep, and then ensure that the green checkmark has appeared after clicking "Prepare Ligand." In step 3, enter the dimensions for the 3D search space for small molecule interaction with the target protein. In field 4, enter the number of random initial conditions to be generated. Finally, in field 5, enter an email that will make results easily accessible.

2.4 Drug Likeness and Toxicity
2.4.1 Drug Properties Predicted by SwissADME

SwissADME is an interface that assesses the drug-likeness of compounds to assist. Information including the solubility, permeation, and other pharmacokinetics of the molecules is outputted (Daina et al., 2017).

To start, SwissADME will require the SMILES format of the compounds. Enter the SMILES for all compounds with each on a separate line. Click "Run" and the 3D structure of the molecule will appear along with information such as molecular mass and hydrogen acceptors and donors. The drug likeness of the molecule is evaluated per rules and any rule violations are noted in the outputs.

2.4.2 Toxicity Predicted by ProTox 3.0

ProTox 3.0 is a website that uses machine learning to predict the toxicity of compounds. Information such as acute and organ toxicity, LD50 (mg/kg), and toxicity class are provided (Banerjee et al., 2024).

Upon reaching the website, enter the SMILES format for the compound into the input box. Select the specific categories for toxicity testing or choose "All" to test all targets. After clicking "Start Tox-Prediction," the LD50 and toxicity class value and all selected target areas and their corresponding toxicity will be displayed. Scroll down to view the toxicity comparison charts.

RESULTS

3.1. Analysis of Binding Sites in TLR4

In drug discovery for small molecule inhibitors of TLR4, potential binding sites for compounds must be identified to ensure that TLR4 is a viable target. Using three different tools maximizes the chances of identifying optimal binding sites for drug development by considering multiple parameters, including geometric, energetic, and chemical properties. DoGSiteScorer's geometric analysis focuses on the physical properties of the binding sites. This tool was used because evaluating the size, shape, and surface properties of binding sites is essential for understanding how well potential inhibitors may interact with TLR4. FTSite's energy-based approach reveals the most energetically favorable binding sites, indicating where protein-ligand interactions are likely strongest. PrankWeb leverages machine learning and considers many different parameters to predict chemically promising sites. Although other tools can be used to identify sites, the above 3 interfaces were selected as they provide an exhaustive approach that ensures that TLR4 has viable binding sites by various evaluation standards.

Table 1. Seventeen binding sites geometrically predicted by DoGSiteScorer for TLR4 (PDB: 2Z64).

Name	Volume (A^3)	Surface Area (A^2)	Drug Score
P_0	631.94	730.88	0.88
P_1	519.51	592.53	0.89
P_10	226.6	594.31	0.58
P_11	184.85	160.34	0.53
P_12	167.38	368.75	0.33
P_13	154.76	263.59	0.37
P_14	132.52	427.98	0.32
P_15	129.22	344.54	0.33
P_16	128.15	211.5	0.18
P_2	382.81	492.8	0.79
P_3	334.46	604.92	0.64
P_4	321.75	690.07	0.52
P_5	275.53	473.04	0.48
P_6	273.2	583.52	0.6
P_7	272.43	367.94	0.48
P_8	249.12	396.74	0.62
P_9	237.18	496.04	0.61
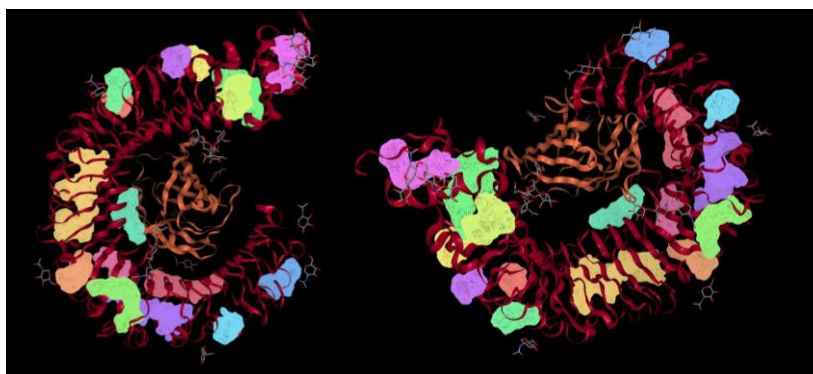
Figure 1. DoGSiteScorer geometrically found 17 binding sites on chain A of TLR4 with PDB 2Z64.
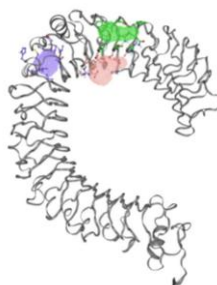
Figure 2. FTSite predicted 3 binding sites on chain A of TLR4 (PDB 2Z64) using an energetic method.
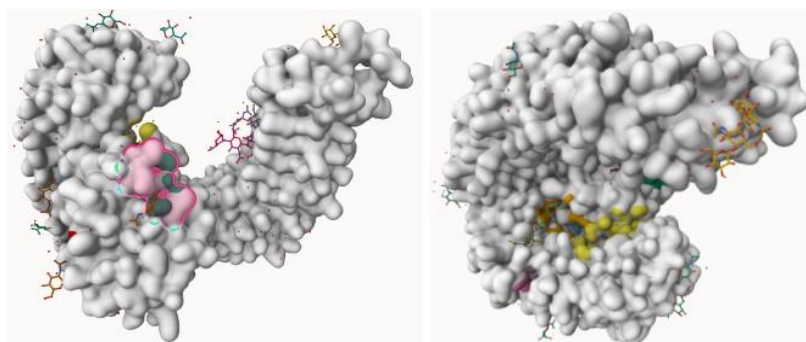
Figure 3. PrankWeb, using machine learning, predicted 10 binding sites on TLR4 (PDB 2Z64).

Table 2. Ten binding sites were predicted by PrankWeb for protein TLR4 with PBD 2Z64.

Pocket Rank	Pocket Score	Number of Amino Acids
1	56.30	32
2	8.87	21
3	4.59	15
4	1.72	10
5	1.60	9
6	1.14	5
7	0.96	7
8	0.87	5
9	0.83	6
10	0.80	6

3.1.1 DoGSiteScorer

DoGSiteScorer identified 17 binding sites for TLR4, indicating that it is a promising target. The volume, surface area, and drug score are provided for each site. The largest binding site is P_0 with a volume of 631.94 A^3, a surface area of 730.88 A^2, and a drug score of 0.88. P_1, although smaller than P_0 with a volume of 519.51 A^3 and a surface area of 592.53 A^2, had the highest drug score of 0.89. Volumes and surface areas of the predicted binding sites ranged from 128.15 A^3(P_16) to 631.94 A^3 and 160.34 A^2 (P_11) to 730.88 A^2, respectively. Drug scores fell between 0.18 (P_16) to 0.89.

3.1.2 FTSite

FTSite detected three viable binding sites represented in purple, pink, and green in Figure 2.

3.1.3 PrankWeb

PrankWeb detected 10 binding sites. The pocket with the highest score had a score of 56.30 and 32 amino acids. Scores in the ten sites were between 0.80 and 56.30 with the number of amino acids ranging from 6 to 32 residues.

Overall, considering that both ProteinPlus (which utilizes the reputable geometric approach) and PrankWeb (which considers many factors through machine learning) predicted 17 and 10 sites, respectively, it was unexpected that FTSite provided only 3 binding sites. This may indicate that some of the binding sites identified by ProteinPlus and PrankWeb had improper hydrophobicity and hydrophilicity balance. For example, the pocket ranked number 3 by PrankWeb proved to be composed of arginine and aspartic acid, 2 highly polar amino acids. FTSite may not have deemed this pocket a binding site if the excessive polarity reduced binding affinity, making it difficult for ligands to bind. Still, at least 3 sites were identified by experimenting using ProteinPlus, FTSite, and PrankWeb.

3.2 Drug Discovery Tools to Generate Pharmacophore Maps and Small Molecule Targets

Pharmacophore maps are crucial in drug discovery as they highlight necessary molecular features indicating biological activity that determines the drug's potential. Key features such as the types and number of interactions between proteins are presented in these maps. In this paper, the website PocketQuery is used to create pharmacophore maps. Virtual screening is then conducted by ZINCPharmer which utilizes a computational method that identifies potential drug candidates that can bind to the TLR4 sites from vast libraries of small molecules.

3.2.1 Identification of Pharmacophore Maps Binding to TLR4 using PocketQuery

PocketQuery generated 16 clusters that had promising scores (determined based on the druggability of the cluster) that were higher than the threshold of 0.7. The top 4 of these clusters were selected and their corresponding information is displayed in Table 3. The highest-ranking cluster scored 0.811032, indicating that promising binding sites on the TLR4 surface were present.

3.2.2 Virtual Screening for Small Molecule Targets using ZINCPharmer

All 16 clusters were virtually screened using ZINCPharmer and the lowest RMSD (root-mean-square-deviation) compounds were selected. Since a lower RMSD score indicates a stronger compound-receptor match, the 20 lowest RMSD candidates were chosen. Several compounds had an RMSD of 0.004, so 3 of these compounds were randomly chosen from clusters 3 and 4.

Table 3. PocketQuery's output of the amino acids, distance, and score of the top 4 clusters of TLR4 (PDB 2Z64).

Cluster	Residues	Distance	Score
1	HIS96; HIS98; ASP99; ASP101	9.6257	0.811032
2	HIS98; ASP99; ASP100; ARG106	10.8619	0.804953
3	HIS98; ASP101	9.6257	0.802837
4	HIS98; ASP99; ASP101	9.6257	0.801867

Table 4. Results of pharmacophore screenings from ZINCPharmer for TLR4 (PDB: 2Z64). The pharmacophore class, spatial coordinates in the model, compound, mass, and RMSD (root-mean-square-deviation) are displayed. The compounds with the 20 lowest RMSDs were selected.

Cluster	Pharmacophore Class	x	y	z	Name	RMSD	Mass
1	Hydrogen Acceptor	-27.76	-8.04	-4.57	ZINC03142646	0.000	525
					ZINC04694172	0.001	402
	Hydrogen Acceptor	-27.89	-14.86	2.96	ZINC08843242	0.001	501
					ZINC91602001	0.001	308
					ZINC10092251	0.002	359
	Hydrophobic	-24.37	-6.89	-3.77	ZINC78631558	0.002	327
					ZINC63786726	0.002	432
					ZINC19583985	0.003	414
					ZINC90107583	0.003	360
					ZINC03305530	0.003	386
2	Hydrogen Acceptor	-27.76	-8.04	-4.57	ZINC09686198	0.000	399
					ZINC14168858	0.003	330
	Hydrogen Acceptor	-32.59	-12.22	3.74	ZINC04139831	0.003	340
					ZINC06441606	0.003	370
					ZINC05032710	0.003	358
	Hydrophobic	-24.37	-6.89	-3.77	ZINC05032516	0.003	354
3	Hydrogen Acceptor	-27.46	-12.72	3.05	ZINC76762626	0.004	358
	Hydrogen Acceptor	-27.89	-14.86	2.96			
	Hydrogen Acceptor	-32.59	-12.22	3.74			
4	Hydrogen Acceptor	-27.46	-12.72	3.05	ZINC92797485	0.003	365
					ZINC12339614	0.004	351
	Hydrogen Acceptor	-27.89	-14.86	2.96	ZINC89512669	0.004	339
	Hydrophobic	-24.37	-6.89	-3.77			

Based on the results, many molecules have a high probability of binding to TLR4. The most promising of them are ZINC03142646 and ZINC09686198 which have RMSD scores of 0, indicating that the two superimposed molecules are perfectly aligned. The other 18 compounds also display a high likelihood of binding to TLR4, with the highest RMSD at a relatively low value of 0.004.

### 3.3 Molecular Docking Results for TLR4

The 3 compounds with the lowest Gibbs Free Energy and therefore the most favorable interactions with TLR4 are ZINC08843242, ZINC03142646, and ZINC04694172. These compounds have a △G of -8.5248, -8.2719, and -7.6852 kcal/mol respectively. These 3 molecules, along with 7 more compounds, will be further investigated due to their △G exceeding -7.5

kcal/mol, proving them to be the 10 most successful candidates with favorable interaction energies

3.4 Drug Likeness Predicted by SwissADME

From SwissDock, the 10 compounds with the lowest △G were selected for SwissADME evaluation. The number of hydrogen bond acceptors and donors, molecular mass, LogP, Lipinski rule violations, and permeability of the blood-brain barrier for each compound are produced. Lipinski's rule states that the compound's molecular weight must be less than 500 g/mol, the number of hydrogen bond donors must not exceed 5, the number of hydrogen bond acceptors must not exceed 10, and the calculated LogP value must not exceed 5 for the molecule's absorption and permeation efficacy.
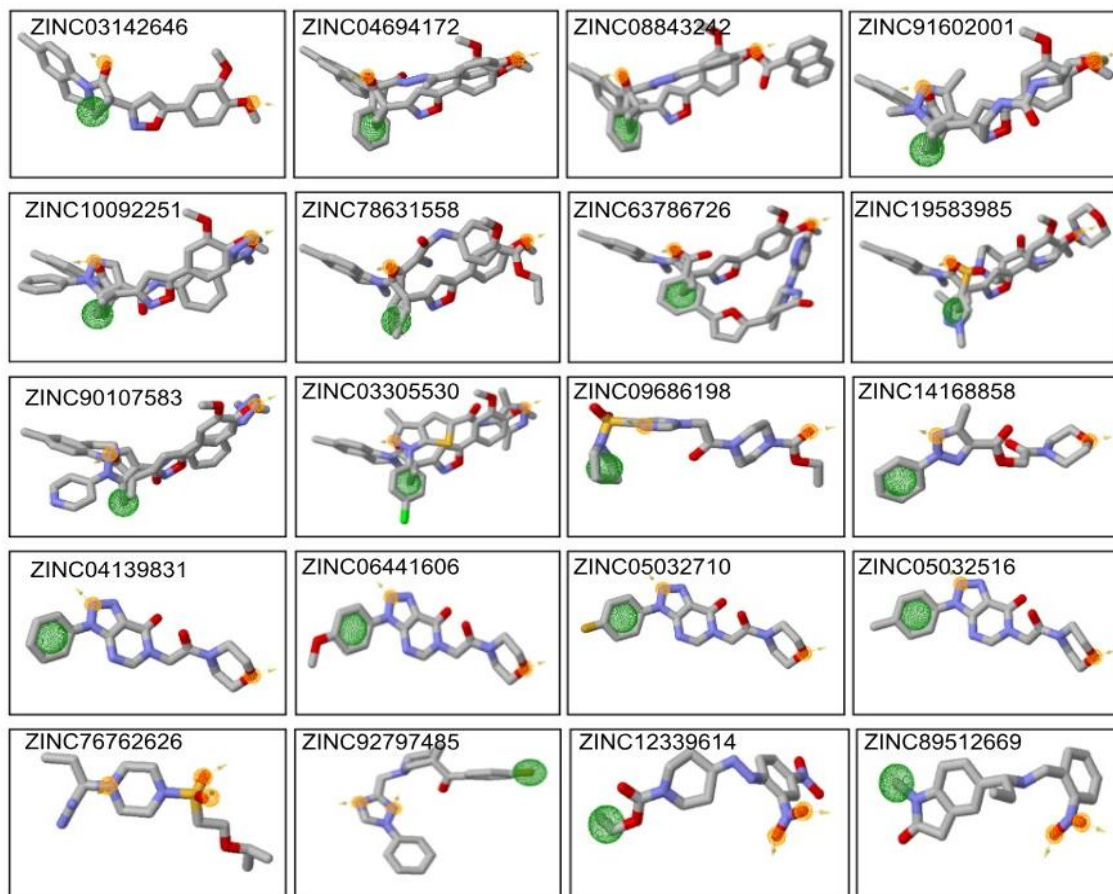
Figure 4. 20 selected molecules from ZINCPharmer for TLR4 inhibition (PDB: 2Z64). Molecules are shown superimposed over their corresponding pharmacophore map.

Table 5. Compound and △G data from SwissDock which modeled compound interaction with TLR4.

Compound	SwissParam Score (△G) (kcal/mol)	Compound	SwissParam Score (△G) (kcal/mol)
ZINC03142646	-8.2719	ZINC09686198	-7.6621
ZINC04694172	-7.6852	ZINC14168858	-7.4757
ZINC08843242	-8.5248	ZINC04139831	-7.5866
ZINC91602001	-7.5032	ZINC06441606	-7.4965
ZINC10092251	-6.9176	ZINC05032710	-7.5028
ZINC78631558	-7.4033	ZINC05032516	-7.4282
ZINC63786726	-7.2505	ZINC76762626	-7.5691
ZINC19583985	-7.6239	ZINC92797485	-7.4294
ZINC90107583	-7.5952	ZINC12339614	-7.3448
ZINC03305530	-7.3271	ZINC89512669	-7.5428

Table 6. Drug likeness of top 10 compounds by SwissADME for inhibition of protein TLR4.

Compound	Hydrogen bond acceptors	Hydrogen bond donors	Mass (g/mol)	LogP value	Number of Lipinski Rule Violations	Blood Brain Barrier Permeant
ZINC08843242	5	2	500.54	3.94	2	No
ZINC03142646	8	2	524.52	3.85	1	No
ZINC04694172	5	2	402.44	3.28	0	No
ZINC09686198	7	0	399.47	2.55	0	No
ZINC19583985	7	1	413.53	3.16	0	No
ZINC90107583	6	1	360.37	2.50	0	No
ZINC04139831	6	0	340.34	2.31	0	No
ZINC76762626	6	0	358.34	2.31	0	No
ZINC89512669	4	1	339.39	2.80	0	Yes
ZINC91602001	3	2	308.42	2.82	0	Yes

Table 7. LD50 (mg/kg), toxicity class ranking, active areas, and probability of being active from ProTox 3.0 are shown for ZINC91602001 which is most suitable for TLR4 inhibition.

LD50 (mg/kg)	Toxicity Class (out of 6)	Active Target	Probability
4580	5	Neurotoxicity	0.58
		Respiratory toxicity	0.64
		Carcinogenicity	0.60
		BBB-barrier	0.60
		GABA receptor	0.51

Surprisingly, the two compounds with the highest △G were the only ones to violate Lipinski's rules. The third through tenth compounds did not violate Lipinski's rule. However, considering that the drug must be absorbed and able to penetrate the blood-brain barrier (BBB) to reach TLR4, additional factors such as solubility, gastrointestinal (GI) absorption, and BBB permeation were also considered. The compound that scored highest across all standards was ZINC91602001 which met Lipinski's rules and was soluble, had a "high" GI absorption, and was a BBB permeant.

3.5 Toxicity of Compound ZINC91602001 Predicted by ProTox 3.0

Since ZINC91602001 has proved to be the most suitable candidate thus far, its toxicity was examined through ProTox 3.0 to ensure that this molecule not

only successfully inhibits TLR4 theoretically but can also prove to be a non-lethal, safe drug administered to humans.

Despite identifying five active target areas, the exhibited toxicity probabilities ranged from 0.51 to 0.64, indicating that concerns are mild as all active probabilities are below the 0.7 threshold. Additionally, the toxicity exhibited in active and all other target areas is less than the active toxicity for average FDA-approved drugs. Combined with the fact that the LD50 is extremely high, meaning that an immense amount of ZINC91602001 would be needed to make the compound lethal, and the toxicity class rating is 5 out of 6, this drug is very likely safe and non-toxic.

CONCLUSION

Alzheimer's is a life-threatening disease that has afflicted millions. This paper uses methods to determine TLR4's binding sites, generate pharmacophore maps, run virtual screening of small molecules, simulate molecular docking, and identify the properties of drug candidates. This process has led to the identification of one promising compound, ZINC91602001. Although its Gibbs Free Energy was higher in comparison to other screened molecules at -7.5032 kcal/mol, placing it at the tenth lowest $\triangle G$ out of the 20 candidates, this compound not only met Lipinski's rule but was also the only molecule to be classified as soluble, have high GI absorption, and the ability to penetrate the BBB which is crucial for its practicality in inhibiting TLR4 in the brain. Overall, ZINC91602001 can be further evaluated through in vitro and in vivo experiments. In the future, cell-based assays can be utilized to determine if ZINC91602001 reduces neuroinflammation in AD models and evaluate its potential to serve as a clinical Alzheimer's antagonist.

REFERENCES

Akira S, Uematsu S, Takeuchi O. Pathogen Recognition and Innate Immunity. Cell. 2006;124(4):783–801. doi: 10.1016/j.cell.2006.02.015.

Al-Ghraiybah NF, Wang J, Alkhalifa AE, Roberts AB, Raj R, Yang E, Kaddoumi A. Glial Cell-Mediated Neuroinflammation in Alzheimer's Disease. Int J Mol Sci. 2022 Sep 12;23(18):10572. doi: 10.3390/ijms231810572. PMID: 36142483; PMCID: PMC9502483.

Bamberger ME, Harris ME, McDonald DR, Husemann J, Landreth GE. A cell surface receptor complex for fibrillar beta-amyloid mediates microglial activation. J Neurosci. 2003 Apr 1;23(7):2665-74. doi: 10.1523/JNEUROSCI.23-07-02665.2003. PMID: 12684452; PMCID: PMC6742111.

Banerjee P, Kemmler E, Dunkel M, Preissner R. ProTox 3.0: a webserver for the prediction of toxicity of chemicals. Nucleic Acids Res. 2024 (Web server issue); NAR.

Bugnon M, Röhrig UF, Goullieux M, Perez MAS, Daina A, Michielin O, Zoete V. SwissDock 2024: major enhancements for small-molecule docking with Attracting Cavities and AutoDock Vina. Nucleic Acids Res. 2024.

Calvo-Rodriguez M, García-Rodríguez C, Villalobos C, Núñez L. Role of Toll Like Receptor 4 in Alzheimer's Disease. Front Immunol. 2020 Aug 26;11:1588. doi: 10.3389/fimmu.2020.01588. PMID: 32983082; PMCID: PMC7479089.

Centers for Disease Control and Prevention. What Is Alzheimer's Disease? 26 Oct. 2020. [Online] Available: https://www.cdc.gov/aging/aginginfo/alzheimers.htm [Accessed: 30 June 2024].

Chen GF, Xu TH, Yan Y, Zhou YR, Jiang Y, Melcher K, Xu HE. Amyloid beta: structure, biology and structure-based therapeutic development. Acta Pharmacol Sin. 2017 Sep;38(9):1205-1235. doi: 10.1038/aps.2017.28. Epub 2017 Jul 17. PMID: 28713158; PMCID: PMC5589967.

Ciesielska A, Matyjek M, Kwiatkowska K. TLR4 and CD14 trafficking and its influence on LPS-induced pro-inflammatory signaling. Cell Mol Life Sci. 2021 Feb;78(4):1233-1261. doi: 10.1007/s00018-020-03656-y. Epub 2020 Oct 15. PMID: 33057840; PMCID: PMC7904555.

Daina A, Michielin O, Zoete V. SwissADME: a free web tool to evaluate pharmacokinetics, drug-likeness and medicinal chemistry friendliness of small molecules. Sci Rep. 2017;7:42717. doi: 10.1038/s41598-017-42817-6.

Duan T, Du Y, Xing C, Wang HY, Wang RF. Toll-Like Receptor Signaling and Its Role in Cell-Mediated Immunity. Front Immunol. 2022 Mar 3;13:812774. doi: 10.3389/fimmu.2022.812774. PMID: 35309296; PMCID: PMC8927970.

2023 Alzheimer's disease facts and figures. Alzheimer's Dement. 19:1598-1695. doi: 10.1002/alz.13016. Available at: https://alz-journals.onlinelibrary.wiley.com/doi/10.1002/alz.13016 [Accessed: 20 June 2024].

Glass CK, Saijo K, Winner B, Marchetto MC, Gage FH. Mechanisms underlying inflammation in neurodegeneration. Cell. 2010 Mar 19;140(6):918-34. doi: 10.1016/j.cell.2010.02.016. PMID: 20303880; PMCID: PMC2873093.

Hur JY. γ-Secretase in Alzheimer's disease. Exp Mol Med. 2022 Apr;54(4):433-446. doi: 10.1038/s12276-022-00754-8. Epub 2022 Apr 8. PMID: 35396575; PMCID: PMC9076685.

J Jendele, Lukas et al. PrankWeb: a web server for ligand binding site prediction and visualization. Nucleic Acids Res. 2019;47(W1). doi: 10.1093/nar/gkz339.

Koes DR, Camacho CJ. PocketQuery: protein-protein interaction inhibitor starting points from protein-protein interaction structure. Nucleic Acids Res. 2012;40(Web Server issue). doi: 10.1093/nar/gks317.

Koes DR, Camacho CJ. ZINCPharmer: pharmacophore search of the ZINC database. Nucleic Acids Res. 2012;40(Web Server issue). doi: 10.1093/nar/gks375.

Kwon HS, Koh SH. Neuroinflammation in neurodegenerative disorders: the roles of microglia and astrocytes. Transl Neurodegener. 2020 Nov 26;9(1):42. doi: 10.1186/s40035-020-00221-2. PMID: 33239064; PMCID: PMC7689983.

Mangalmurti A, Lukens JR. How neurons die in Alzheimer's disease: Implications for neuroinflammation. Curr Opin Neurobiol. 2022 Aug;75:102575. doi: 10.1016/j.conb.2022.102575. Epub 2022 Jun 10. PMID: 35691251; PMCID: PMC9380082.

Ngan CH, Kryshtafovych A, Chen S, Wu Y, Lai Y, Borhani DW, et al. FTSite: high accuracy detection of ligand binding sites on unbound protein structures. Bioinformatics. 2012;28(2):286-7. doi: 10.1093/bioinformatics/btr643.

Płóciennikowska A, Hromada-Judycka A, Borzęcka K, Kwiatkowska K. Co-operation of TLR4 and raft proteins in LPS-induced pro-inflammatory signaling. Cell Mol Life Sci. 2015 Feb;72(3):557-581. doi: 10.1007/s00018-014-1762-5. Epub 2014 Oct 22. PMID: 25332099; PMCID: PMC4293489.

Rajesh Y, Kanneganti TD. Innate Immune Cell Death in Neuroinflammation and Alzheimer's Disease. Cells. 2022 Jun 10;11(12):1885. doi: 10.3390/cells11121885. PMID: 35741014; PMCID: PMC9221514.

Röhrig UF, Goullieux M, Bugnon M, Zoete V. Attracting Cavities 2.0: improving the flexibility and robustness for small-molecule docking. J Chem Inf Model. 2023;63(4):1445-1452. doi: 10.1021/acs.jcim.2c01471.

Scheltens P, De Strooper B, Kivipelto M, Holstege H, Chételat G, Teunissen CE, Cummings J, van der Flier WM. Alzheimer's disease. Lancet. 2021 Apr 24;397(10284):1577-1590. doi: 10.1016/S0140-6736(20)32205-4. Epub 2021 Mar 2. PMID: 33667416; PMCID: PMC8354300.

SwissDock 2024: major enhancements for small-molecule docking with Attracting Cavities and AutoDock Vina. Nucleic Acids Res. 2024.

Volkamer A, Kuhn D, Rippmann F, Sticht H. Combining global and local measures for structure-based druggability predictions. J Chem Inf Model. 2012;52(2):360-72. doi: 10.1021/ci200507h.

Wu L, Xian X, Xu G, Tan Z, Dong F, Zhang M, Zhang F. Toll-Like Receptor 4: A Promising Therapeutic Target for Alzheimer's Disease. Mediators Inflamm. 2022 Aug 21;2022:7924199. doi: 10.1155/2022/7924199. PMID: 36046763; PMCID: PMC9420645.

Yang J, Wise L, Fukuchi KI. TLR4 Cross-Talk With NLRP3 Inflammasome and Complement Signaling Pathways in Alzheimer's Disease. Front Immunol. 2020 Apr 23;11:724. doi: 10.3389/fimmu.2020.00724. PMID: 32391019; PMCID: PMC7190872.

Zusso M, Lunardi V, Franceschini D, Pagetta A, Lo R, Stifani S, Frigo AC, Giusti P, Moro S. Ciprofloxacin and levofloxacin attenuate microglia inflammatory response via TLR4/NF-kB pathway. J Neuroinflammation. 2019 Jul 18;16(1):148. doi: 10.1186/s12974-019-1538-9. PMID: 31319868; PMCID: PMC6637517.

Publisher's Note
IJLSCI remains neutral with regard to jurisdictional claims in published maps and institutional affiliations.

Correspondence and requests for materials should be addressed to Vemulapalli Sindhu.

Peer review information
IJLSCI thanks the anonymous reviewers for their contribution to the peer review of this work. A peer review file is available.

Reprints and permissions information is available at https://www.ijlsci.in/reprints